Automotive Science and Engineering, Vol. 13, No. 4, (2023), 4225-4235

Iran University of Science and Technology

Automotive Science and Engineering

Journal Homepage: ase.iust.ac.ir

ISSN: 2008-9899

Finite element analysis of an adhesively bonded Al\CFRP square section under axial & oblique loading

H. Ghasempoor [1], A. Keshavarzi [2], H. Saeidi Googarchin [3*]

[1] Master Student at School of Automotive Engineering, Iran University of Science and Technology, Tehran, Iran; hamidreza_ghasempoor@auto.iust.ac.ir

[2] PhD Student at School of Automotive Engineering, Iran University of Science and Technology, Tehran, Iran; ali_keshavarzi@auto.iust.ac.ir

[3] Faculty at School of Automotive Engineering, Iran University of Science and Technology, Tehran, Iran; hsaeidi@iust.ac.ir

ARTICLE INFO

Article history:

Received: 1 Sep 2023

Accepted: 28 Oct 2023

Published: 13 Nov 2023

Keywords:

Carbon fiber reinforced plastic (CFRP)

Thin-walled structures

Specific energy absorption (SEA)

Crashworthiness

Oblique loading

A B S T R A C T

The utilization of adhesively bonded square sections (ABSS) serves to enhance energy absorption and specific energy absorption (SEA) when subjected to oblique loading. Finite element models utilizing LS-DYNA were constructed in order to examine the deformation mode and load-displacement characteristics of ABSS and hybrid aluminum/carbon fiber reinforced polymer models. Subsequently, an evaluation was conducted on the general parameter pertaining to crashworthiness and the capacity for absorption of energy. The results reveal that an increase in the quantity of Carbon Fiber Reinforced Polymer (CFRP) layers within the stacking sequence of [0,90] affords enhanced potential for energy absorption. Conversely, the stacking sequence of [90] exhibits an incongruity with this trend, and achieves superior energy absorption capacity with a count of 4 CFRP layers rather than 8. The present study indicates that carbon fiber reinforced polymer (CFRP) possessing a stacking sequence of [90] exhibits superior energy absorption capacity under both axial and oblique loading conditions at an inclination angle of 10 degrees. In contrast, the use of eight layers of CFRP with a stacking sequence of [0, 90] is found to yield better performance in achieving both axial and oblique loading up to 10 degrees.

1. Introduction

During the preceding twenty years, thin-walled setups have been broadly utilized as energy-absorbing structures in numerous building areas including the aforementioned industries, including but not limited to aerospace, nautical, maritime, automotive, and rail transportation, comprise a diverse array of sectors within the broader field of transportation and mobility. The pursuit of lighter and safer energy-absorbing configurations has significantly intensified due to the recent increase in awareness of their outstanding durability, productivity, and ever-increasing concerns about fuel consumption, environmental pollution, and crash safety [1]. The safety of collisions is a paramount concern in the design of automobiles. It is projected that vehicular configurations will surveil individuals and/or commodities through the conversion of the majority of kinetic energy from a collision into various forms of manageable energy. The utilization of lightweight thin-walled structures as crashworthy structures is commonplace. Moreover, a multitude of sophisticated

*Corresponding Author
Email Address: hsaeidi@iust.ac.ir
https://doi.org/10.22068/ase.2023.652

[DOI: 10.22068/ase.2023.652]

engineering materials, including aluminum alloys and high-strength steels, have been integrated into the design of these structural arrangements. This assertion is supported by a source reference [2].

The onset of an unintended restraint condition in the operational framework of vessels necessitates the implementation of suitable mechanisms for quantifying the extent of the damage resulting from collisions with other ships or stationery or drifting objects. Several auditing methods, including expository, numerical, and test protocols, have been employed or are currently being utilized to evaluate the factors contributing to dispatch collisions. This paper examines the strategies that have been employed with respect to plan requirements and their evolution over the past six decades. The present study endeavors to underscore the difficulties being confronted by researchers in the domain of transport accident recreation and the current state of their expertise. As such, it seeks to encourage an in-depth understanding of this evolving field [3]. Stand up to the conventional strategies of associations (i.e., welds, jolts, or bolts), the adhesion technology has major points of interest, including the joint exhibit a commendable level of flexibility in its connection, Improved distribution of stress is deemed desirable, and fatigue resistance. The prevalent utilization of current lightweight objects in the automotive sector has led to the increasing prominence of adhesive bonding between dissimilar materials. Currently, AL and CFRP are the primary lightweight materials employed in the automotive sector [4]. In actual vehicular accidents, the crash boxes are often exposed to non-perpendicular forces. The bumper framework has been deemed appropriate for the management of a stack subject to an impacting angle of up to 30 degrees. However, objects can exhibit intricate deformation patterns when subjected to oblique loads. Given a small oblique load, it may be observed that the segment exhibits a progressive crush deformation mode. However, when subjected to oblique loads at a critical angle, the region undergoes global bending instead of dynamic smashing, resulting in a reduction in energy absorption capacity [5].

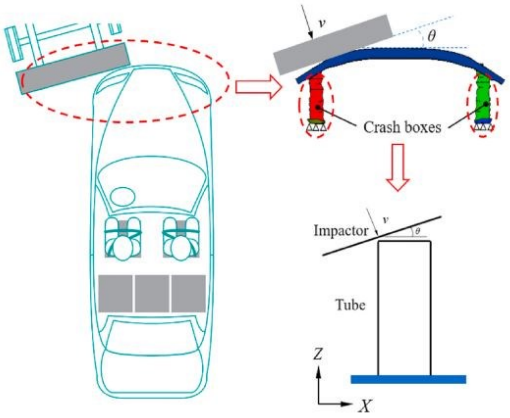

Figure 1. Oblique energy absorption by crash boxes [5]

For Adhesively fortified arrangements utilizing Al and CFRP, simple lap joint (SLJ) is accepted as of late. In their investigation, Liu [6] and colleagues examined the failure mechanisms of the joints between carbon fiber reinforced polymer (CFRP) and aluminum (Al) subsequent to transverse pre-impact and axial post-tension application. Zheng et al. [4] investigates the influence of elevated temperature, in conjunction with fixed loading, on the mechanical response of single-lap joints (SLJs) fabricated using various materials, including aluminum alloy (AL), carbon amalgam (AL) and carbon fiber-reinforced plastic (CFRP). Sun [7] and colleagues conducted a comprehensive investigation of mechanical behaviors and failure mechanisms exhibited by various joint strategies involving dissimilar materials, including rivet joints, bolt joints, and hybrid joints combining rivet and bolt components.

Other articles including; the fatigue behavior [8] of Carbon Fiber Reinforced Polymer (CFRP)/Aluminum (Al) single lap joints through an experimental approach utilizing Digital Image Correlation (DIC) measurement. Another article endeavors to examine the hygrothermal impacts [9] on the residual mechanical properties of dissimilar adhesive joints by utilizing bulk specimens, Al, and CFRP substrates.

Hybrid tubes, which incorporate metallic materials possessing desirable toughness, and economic viability, along with CFRP boasting superior specific strength and stiffness, represent a fitting solution for effectively

[DOI: 10.22068/ase.2023.652]

addressing this challenge. Wang et al. [10] investigated the mechanical properties of steel and glass fiber reinforced polymer. The sections were evaluated through the implementation of both quasi-static and dynamic experiments. According to the findings of the experiment, Sun et al. [11] showed the findings indicate that the hybrid circular tubes demonstrated a greater capacity for energy absorption in comparison to both the individual metal tube and the CFRP tube. The previously cited study pertaining to hybrid square tubes primarily addressed the crashworthiness efficacy of slender walled frameworks subjected to axial crushing.

A variety of novel structures have been proposed by scholars for improving the energy absorption capabilities of slender structures subjected to oblique loading. Such structures encompass, among others, tapered tubes [12] and metal tubes with non-uniform wall thickness [13]. The predominant area of focus pertaining to oblique loading conditions in research lies in the application to metallic tube materials. As demonstrated by Li [14], An investigation into the comparative specific energy absorption properties of circular tubes with variable thickness and tapered tubes, subject to varying loading angles, determined that the former demonstrated a superior SEA value. Tabacu [15] conducted an empirical investigation to elucidate the deformation mechanism displayed by a multi-cellular tube under oblique loading conditions. Subsequently, a predictive model for assessing the average force was proposed. Pirmohammad [16] undertook an analysis of polygonal structures fortified with internal ribs for performance evaluation. The external façade displayed an assortment of polygonal geometries that incorporated triangular, square, hexagonal, octagonal, and decagonal elements, as well as circular segments. The numerical outcomes demonstrate that the energy absorption proficiency exhibited by multi-cellular tubes featuring decagonal and octagonal cross-sectional configurations surpasses other variants. The goal of this article was to investigate structural crashworthiness and energy absorption of locally reinforcement adhesively bonded Al with CFRP under oblique loading.

The present study is centered on the examination of the influence that modifications to the oblique angle, ply angle, and the quantity of carbon fiber reinforced polymer (CFRP) layers may have on the crashworthiness of structures. The accomplishment was realized via the utilization of the nonlinear finite element simulation software, LS-DYNA. To attain a comprehensive comprehension of the diverse factors and their potential consequences, the investigation took into account axial and oblique loading scenarios.

2. Design of ABSS

2.1. Description of the ABSS

Knowing the advantages of adhesive bonding, we can create adhesively bonded square section (ABSS). As shown in Fig. 2. The ABSS comprised by two Al U Shape with thickness of 1 mm, adhesively attached to each other using Araldite® 2015.The ABSS with dimensions of height h = 200 mm, a = 60 mm. Double Al U shapes adhesive 30 mm from Side of the square to each other to create ABSS.

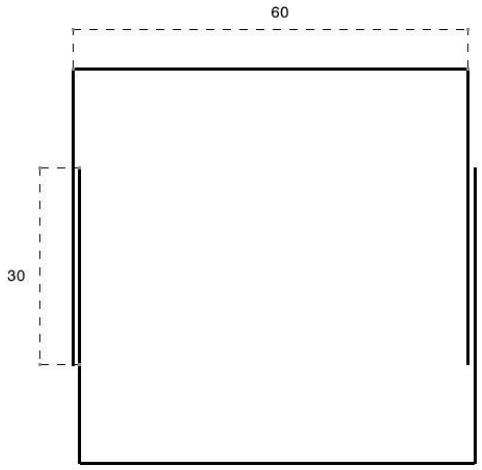

Figure 2. ABSS Cross-section view

Using four CFRP 14×14×200 mm outside corners of ABSS to create locally reinforcement hybrid model as seen in figure 3.

[DOI: 10.22068/ase.2023.652]

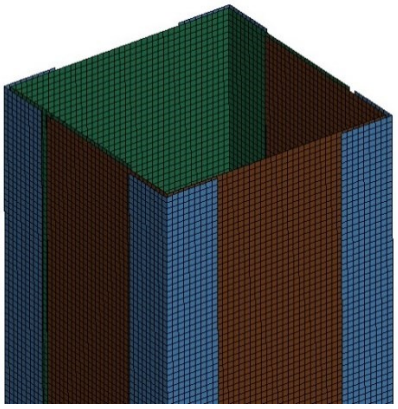

Figure 3. finite element model of outside locally reinforcement

2.2. Materials

In this study Al 3105 which is used for ABSS has the following properties; $\rho = 2.7\ \mathrm{g/cm^3}$, $E = 69\ \mathrm{GPa}$, $v = 0.33$, $\sigma_y = 145\ \mathrm{MPa}$ and the stress-strain curve of aluminum exhibited in Figure 4. is representative of the engineering properties of this material.

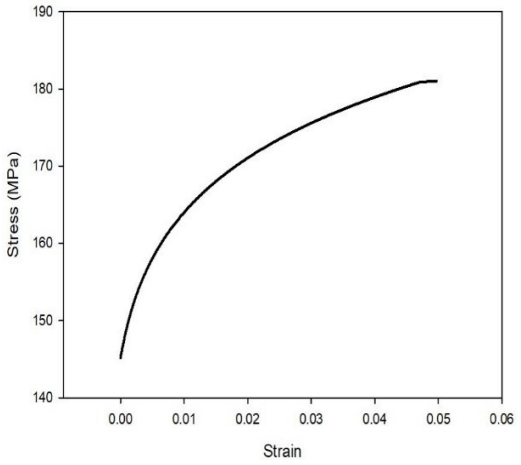

Figure 4. Engineering stress-strain curve for the aluminum alloy 3105 [17]

The adhesive Araldite® 2015 was employed for the purpose of this study, and a comprehensive depiction of material properties of both the adherend and adhesive can be found in Table 1.

Table 1. Material properties of Al 3105 [17] and Araldite 2015 [18].

Materials properties	Materials	
	Al 3105	Araldite 2015
Young's modulus (GPa)	69	1.85 ±0.21
Poisson's ratio	0.33	0.33
Yield stress (MPa)	145	12.63 ±0.61
Ultimate stress (MPa)	181	21.63 ±1.61

The ABSS with CFRP was reinforced using a unidirectional carbon fiber prepreg, of the T300 variant. Table 2 presents the properties of carbon fiber reinforced polymer (CFRP) utilized in the ABSS hybrid model.

Table 2. The material parameters of T300 have been additionally incorporated into the hybrid model, as documented in reference [19].

	Tension		Compression		
Properties	Longitudinal	Transverse	Longitudinal	Transverse	Shear
Density(kg/m^3)	1600				
Young's modulus (MPa)	154000	8650	144000	10300	4680
Ultimate stress (MPa)	2356	34	1119	186	64.78
Poisson's ratio	0.35	0.03	0.288		

2.3. Finite element (FE) model

The finite element models were developed and subsequently analyzed using the LSDYNA software for explicit non-linear finite element analysis. As illustrated in Figure 5, The lower nodes of the ABSS have been fully secured to the lower plate. The upper plate's movement towards the section occurred at a velocity denoted as V_0 = 2.4 m/s as indicated by reference [19]. The impact was carried out at distinct crushing angles designated as θ, which were set at values of 0° and 10°.

[DOI: 10.22068/ase.2023.652]

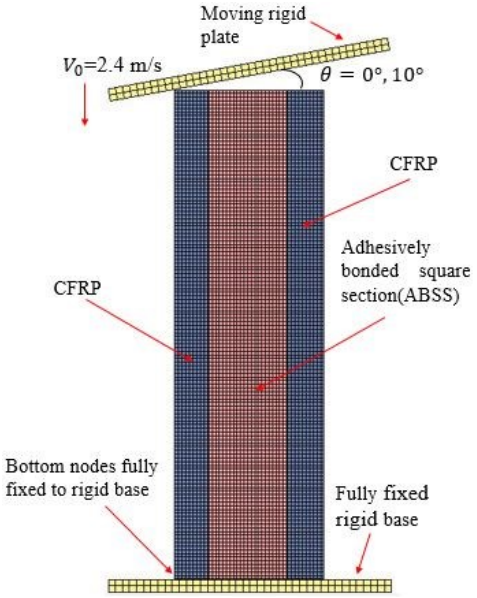

Figure 5. Finite element model of outside reinforcement of ABSS.

A study was conducted to investigate the influence of mesh size on the accuracy of simulation results and computational efficiency of Finite Element (FE) modeling of ABSS. Specifically, three distinct element sizes were examined in the present investigation. There was no statistically significant difference in the dimensions of elements with measurements of 1.0 mm * 1.0 mm and 1.5*1.5 mm. As such, implementing a simulation with a reduced mesh size would not result in enhanced precision but would rather escalate the computational duration and costs involved. Therefore, the dimensions of the mesh can be characterized as 1.5 mm × 1.5 mm. In this study, the FE modeling of both ABSS and hybrid models was accepted, with a focus on utilizing a mesh size of 3 mm * 3 mm for the upper and lower plates. The present study involved the development of an ABSS model utilizing Belytschko-Tsay shell elements consisting of two integration points across the thickness. Furthermore, the hybrid model employed a specific number of layers in accordance with the ABSS requirements. The weight of each ABSS in numerical simulation is 196 g and hybrid model are 236 gr.

The study employed the "automatic surface-to-surface" technique for simulating the interaction between the upper plate and the tube. The simulation technique of "Automatic single surface" was employed to model the phenomenon of self-contact among substrates under compression. The aforementioned ABSS was instituted through the utilization of a bilinear elastic-plastic material model, wherein strain was integrated as a crucial parameter. In the present study, the LS-DYNA software utilized material model 24 for the purpose of investigating hardening processes. In LS-DYNA, the material MAT54 was utilized to replicate the properties of CFRP. The thickness of CFRP assumed equal to Al thickness.

The connection between two aluminum (Al) U shapes is established through the application of the Araldite model. In this particular model, CONTACT_AUTOMATIC_SURFACE_TO SURFACE_TIEBREAK method is employed, ensuring that a defined segment is assigned to each aluminum component. Additionally, the cohesive zone model properties utilized in this study were obtained from previous research efforts [18]. The present investigation sought to assess the failure characteristics of CFRP through the utilization of the Chang-Chang criterion. Additionally, the contact between an ABSS and the CFRP was established through the utilization of the method algorithm CONTACT_AUTOMATIC_ONE_WAY_S URFACE_TO_SURFACE_TIEBREAK. The values appointed for both the static and dynamic coefficient of friction in all contact models were 0.3 and 0.2, respectively. The models were accomplished through computational means utilizing a central processing unit (CPU) with an Intel Core (TM) i5 6800 running at 3.20 GHz and a random-access memory (RAM) capacity of 16.0GB. The estimated computational duration ranged from five to eight hours, contingent upon the distinctive model.

3. Numerical analysis

3.1. Crashworthiness indicators

The evaluation of the crashworthiness of hybrid square tubes under oblique loading typically involves the utilization of three distinct indicators, namely: One commonly utilized measure for evaluating the effectiveness of energy dissipation during compression is energy absorption (EA). " The current notion concerns the computation of the

[DOI: 10.22068/ase.2023.652]

integration of the force of compression over the range of displacement." namely

$$EA = \int_0^{\delta} F(x)dx \quad (1)$$

The equation involves the variable F(x), which represents the instantaneous force that is exerted during the compression process of crushing. The symbol δ represents the complete displacement resulting from a compression process.

The calculation of the mean crushing force (MCF) for an entire section entail determining the proportion of energy dissipated to the total displacement incurred throughout the entirety of the crushing process. This measure is commonly utilized in academic research and engineering contexts to evaluate the resistance of various materials and structures to compression.

$$MCF = \frac{1}{\delta}\int_0^{\delta} F(x)dx \quad (2)$$

The notion of specific energy absorption (SEA) pertains to the measurement of energy absorbed in relation to the mass of a given section, in the course of compression. This parameter can be measured through the use of standardized techniques.

$$SEA = \frac{\int_0^{\delta} F(x)dx}{m} \quad (3)$$

The symbol "m" is representative of the mass attributed to the hybrid square. A superior energy absorption capacity is exhibited by a higher specific energy absorption (SEA) value.

3.2. Crashworthiness analysis of ABSS and hybrid model

3.2.1. Outcomes of ABSS under axial and oblique loading

ABSS with thickness t_m= 1 mm were considered to study crashworthiness indicators under two different loading angles. The final transformation of ABSS under axial loading is depicted in Figure 6. The tubes demonstrate a consistent deformation pattern when subjected to θ = 0° (uniaxial loading) and θ = 10°.

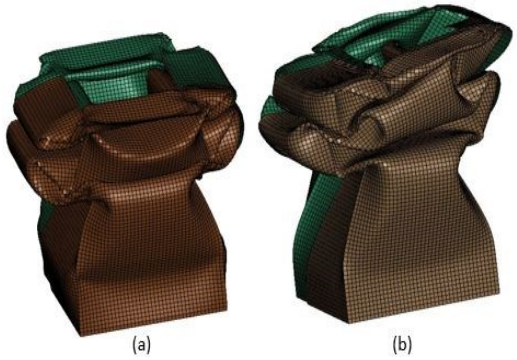

Figure 6. deformation mode of ABSS under (a) axial loading (θ = 0°), (b) oblique loading (θ = 10°)

Figure 7 presents a visual representation that depicts the crashworthiness diagram of the ABSS, as subjected to both axial and oblique loading conditions. When θ increases to 10 °, the energy absorption reduced compare to axial loading.

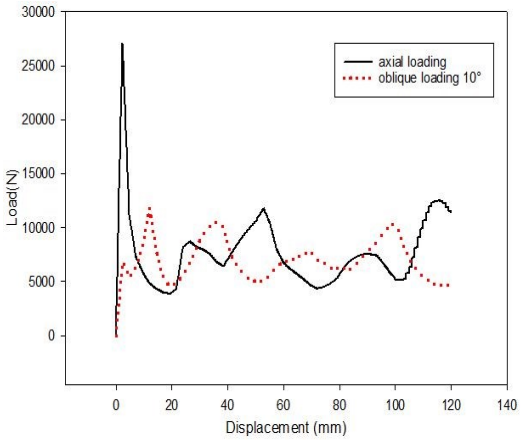

Figure 7. the load-displacement diagram of ABSS subjected to straight and oblique loading

3.2.2. Results of outside reinforcement model under axial and oblique loading

Final deformations of hybrid model with; t_m= 1 mm, t_c= 1 mm, two layers of CFRP with ply angle of [90] were showed in Fig 8. And The results presented in Fig 9.

[DOI: 10.22068/ase.2023.652]

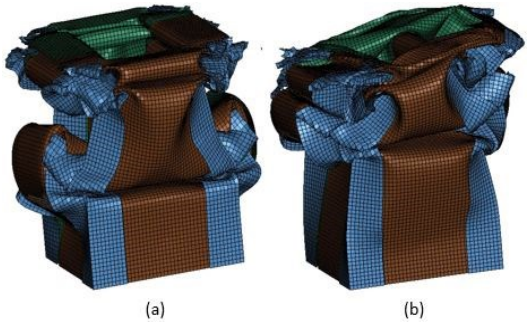

Figure 8. deformation mode of outside reinforcement model under (a) axial loading (θ = 0°), (b) oblique loading (θ = 10°)

We can see the modes of failure and fractures of CFRP in figure 8.

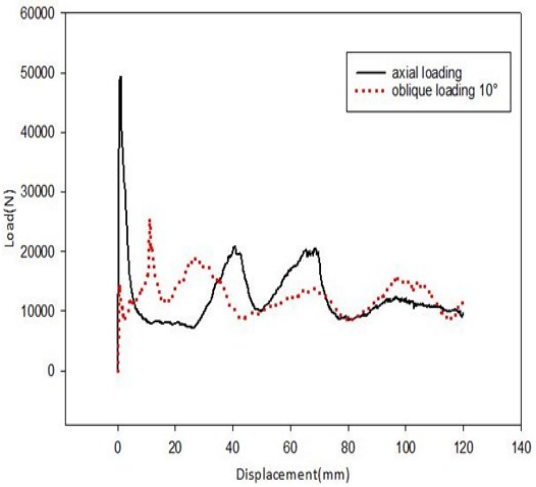

Figure 9. the load-displacement curve of outside hybrid model under axial and oblique loading

The hybrid ABSS exhibits a higher initial peak force due to CFRP compared to ABSS while the total energy absorption of the hybrid model is higher than the ABSS model because of changes in deformation modes. As it is evident, the higher peak force is undesirable for the crashworthiness capability. With adding a trigger in a hybrid model, the initial peak force will be reduced. Also, consider that the increase in total energy absorption can retrieve the amount of energy absorption.

3.3. Parametric studies on hybrid model

3.3.1. Comparison of SEA in ABSS and hybrid model

Using Sigma Plot; macros-area below the curve, the amount of EA (total energy absorption) is calculated from load-displacement curve which we obtain from ls-dyna output.

Table3. Comparison of Specific energy absorption (SEA) and Total energy absorption (EA) in different samples

Samples	M (gr)	EA (KJ)	SEA (KJ/Kg)
Axial ABSS	196	0.921	4.699
Oblique ABSS	196	0.835	4.260
Axial Hybrid model	236	1.505	6.377
Oblique Hybrid model	236	1.499	6.352

As it is obvious from the table, Hybrid models exhibit better energy absorption capacity in both axial and oblique loading.

3.3.2. Effect of different ply angle

The study successfully demonstrated that the crushing characteristics of CFRP layers were significantly affected by the angle of the fibers. The hybrid structure was subjected to an axial loading condition, as reported by reference [20]. The primary objective of this study was to assess the impact of different stacking sequences [0,90], [90] on the crushing characteristics of a hybrid tube under axial and oblique loading conditions. The aluminum wall and CFRP layers were of uniform thickness, measuring 1.0 mm, and were subjected to experimental investigation. The simulation outcomes pertaining to the hybrid tubes, featuring distinct stacking sequences of CFRP layers, have been illustrated in Figure 10.

[DOI: 10.22068/ase.2023.652]

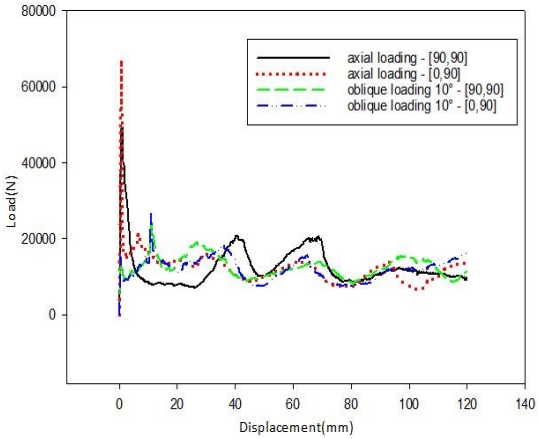

Figure 10. Load-displacement for two layers CFRP in hybrid model under axial and oblique loading

Using two layers of CFRP in model, stacking sequence of [90] provide better result in axial and oblique loading.

In four layers, the stacking sequence of [0,90] shows better crashworthiness performance in oblique loading compared with stacking sequence of [90].

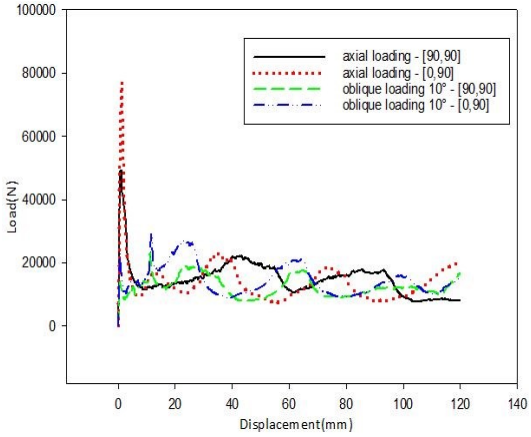

Figure 11. Load-displacement for four layers CFRP in hybrid model under axial and oblique loading

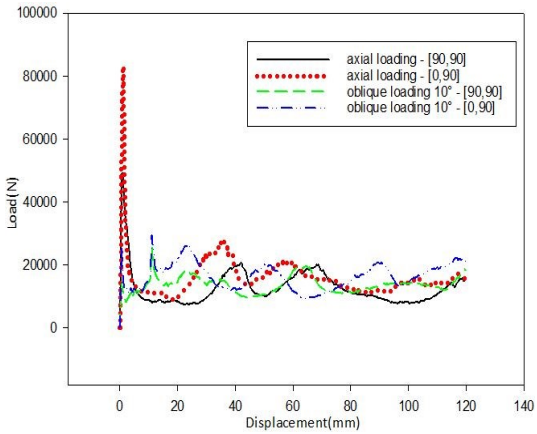

Figure 12. Load-displacement for eight layers CFRP in hybrid model

As we can see in figure 12 with increasing the numbers of CFRP layers, stacking sequence of [0,90] has better performance in crashworthiness.

3.3.3. Effect of number of layers

Three different number of layers; 2,4,8 for CFRP were used while the CFRP thickness t_c remain the same equal to 1 mm. The results of crash simulation for hybrid tubes with a stacking sequence of [90] under axial loading showed in fig.13. The augmentation in the Carbon Fiber Reinforced Polymer (CFRP) layer does not appear to have an impact on the collective deformation patterns exhibited by the hybrid tube with 2 layers and 8 layers of CFRP, but successfully improve specific energy absorption (SEA) by 4 layers of CFRP.

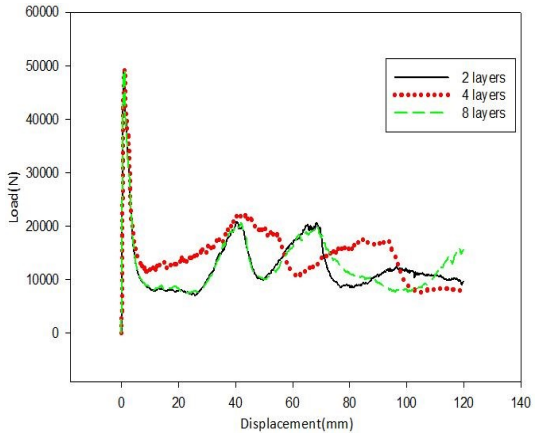

Figure 13. Number of layers in hybrid model with stacking sequence of [90] under axial loading

[DOI: 10.22068/ase.2023.652]

The outcomes pertaining to the hybrid tubes featuring a stacking sequence of [90] under axial loading have been illustrated in Figure 13.

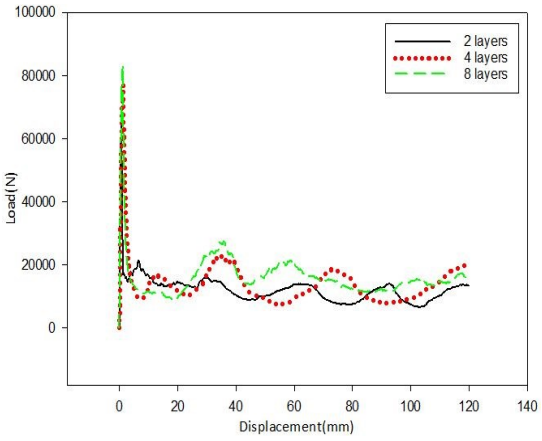

Figure 14 . the quantity of layers in a hybrid model with the stacking sequence [0,90] under the influence of an axial load

the quantity of layers in hybrid model in oblique loading is showed in figure 15 and figure 16.

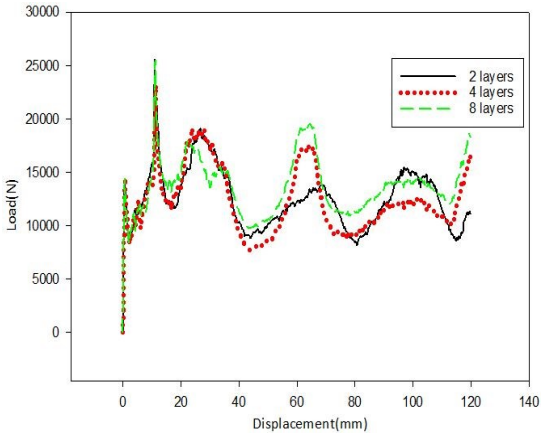

Figure 15. the quantity of layers in hybrid model with stacking sequence of [90] under oblique loading

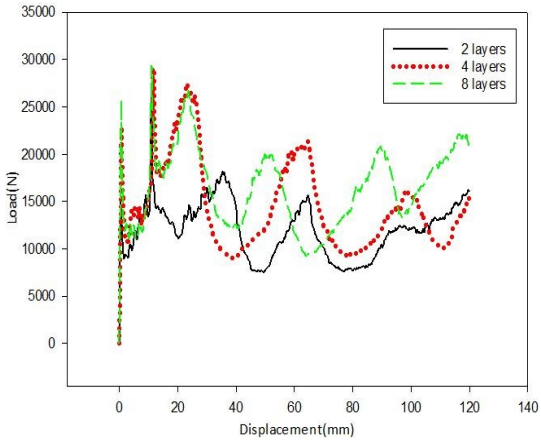

Figure 16. the quantity of layers in hybrid model with stacking sequence of [0,90] under oblique loading

4. Conclusions

One widely acknowledged method for augmenting the energy absorption and Specific Energy Absorption (SEA) of thin-walled structures, which are exposed to axial and oblique loading scenarios, involves the utilization of adhesively bonded square section (ABSS). The present investigation endeavors to examine the crashworthiness of ABSS and hybrid tubes subjected to oblique loading conditions, utilizing simulation techniques. In this article two ply angle [0,90] and [90] with three numbers of CFRP layers, including 2, 4, and 8 layers, were used and presented, and then the effect of the oblique angle in crashworthiness was compared. Stacking sequence of [90] has better results in overall crashworthiness and the results presented.

Declaration of Conflicting Interests

The author(s) declared no potential conflicts of interest with respect to the research, authorship, and/or publication of this article.

Acknowledgements

I would like to thank all the members of the Structures Laboratory of the Iran University of Science and Technology for their help in the realization of this research.

[DOI: 10.22068/ase.2023.652]

References

[1] G. Sun, D. Chen, G. Zhu, and Q. Li, "Lightweight hybrid materials and structures for energy absorption: A state-of-the-art review and outlook," *Thin-Walled Struct.*, vol. 172, no. June 2021, p. 108760, 2022, doi: 10.1016/j.tws.2021.108760.

[2] G. Sun, X. Guo, S. Li, D. Ruan, and Q. Li, "Comparative study on aluminum/GFRP/CFRP tubes for oblique lateral crushing," *Thin-Walled Struct.*, vol. 152, no. August 2019, p. 106420, 2020, doi: 10.1016/j.tws.2019.106420.

[3] M. Samuelides, "Recent advances and future trends in structural crashworthiness of ship structures subjected to impact loads," *Ships Offshore Struct.*, vol. 10, no. 5, pp. 488–497, 2015, doi: 10.1080/17445302.2015.1009287.

[4] G. Zheng, H. Wang, X. Han, and W. Li, "Mechanical behavior of AL / CFRP single-lap joint subjected to combined thermal and constant loading," *J. Adhes.*, vol. 00, no. 00, pp. 1–19, 2019, doi: 10.1080/00218464.2019.1667237.

[5] J. Zhang, D. Zheng, B. Lu, and T. Zhang, "Energy absorption performance of hybrid cross section tubes under oblique loads," *Thin-Walled Struct.*, vol. 159, no. May 2020, 2021, doi: 10.1016/j.tws.2020.107133.

[6] X. Liu, X. Shao, Q. Li, and G. Sun, "Failure mechanisms in carbon fiber reinforced plastics (CFRP) / aluminum (Al) adhesive bonds subjected to low-velocity transverse pre-impact following by axial post-tension," *Compos. Part B Eng.*, vol. 172, pp. 339–351, 2019, doi: 10.1016/j.compositesb.2019.04.036.

[7] G. Sun, X. Xia, X. Liu, Q. Luo, and Q. Li, "On quasi-static behaviors of different joint methods for connecting carbon fiber reinforce plastic (CFRP) laminate and aluminum alloy," *Thin-Walled Struct.*, vol. 164, no. January, p. 107657, 2021, doi: 10.1016/j.tws.2021.107657.

[8] Z. He, Q. Luo, Q. Li, G. Zheng, and G. Sun, "Fatigue behavior of CFRP / Al adhesive joints — Failure mechanisms study using digital image correlation (DIC) technique Thin-Walled Structures Fatigue behavior of CFRP / Al adhesive joints — Failure mechanisms study using digital image correlation (DI," *Thin-Walled Struct.*, vol. 174, no. March, p. 109075, 2022, doi: 10.1016/j.tws.2022.109075.

[9] G. Zheng *et al.*, "Thin-Walled Structures On failure mechanisms in CFRP / Al adhesive joints after hygrothermal aging degradation following by mechanical tests," *Thin-Walled Struct.*, vol. 158, no. August 2020, p. 107184, 2021, doi: 10.1016/j.tws.2020.107184.

[10] X. G. Wang, J. A. Bloch, and D. Cesari, "Static and Dynamic Axial Crushing of Externally Reinforced Tubes," *Proc. Inst. Mech. Eng. Part C J. Mech. Eng. Sci.*, vol. 206, no. 5, pp. 355–360, 1992, doi: 10.1243/PIME_PROC_1992_206_138_02.

[11] G. Sun, Z. Wang, J. Hong, K. Song, and Q. Li, "Experimental investigation of the quasi-static axial crushing behavior of filament-wound CFRP and aluminum/CFRP hybrid tubes," *Compos. Struct.*, vol. 194, no. January, pp. 208–225, 2018, doi: 10.1016/j.compstruct.2018.02.005.

[12] S. E. Alkhatib, F. Tarlochan, A. Hashem, and S. Sassi, "Collapse behavior of thin-walled corrugated tapered tubes under oblique impact," *Thin-Walled Struct.*, vol. 122, no. October 2017, pp. 510–528, 2018, doi: 10.1016/j.tws.2017.10.044.

[13] X. Zhang and H. Zhang, "Relative merits of conical tubes with graded thickness subjected to oblique impact loads," *Int. J. Mech. Sci.*, vol. 98, pp. 111–125, 2015, doi: 10.1016/j.ijmecsci.2015.04.013.

[14] G. Li, F. Xu, G. Sun, and Q. Li, "A comparative study on thin-walled structures with functionally graded thickness (FGT) and tapered tubes withstanding oblique impact loading," *Int. J. Impact Eng.*, vol. 77, no. March,

[DOI: 10.22068/ase.2023.652]

pp. 68–83, 2015, doi: 10.1016/j.ijimpeng.2014.11.003.

[15] S. Tabacu, "Analysis of circular tubes with rectangular multi-cell insert under oblique impact loads," *Thin-Walled Struct.*, vol. 106, pp. 129–147, 2016, doi: 10.1016/j.tws.2016.04.024.

[16] S. Pirmohammad and H. Nikkhah, "Crashworthiness investigation of bitubal columns reinforced with several inside ribs under axial and oblique impact loads," *Proc. Inst. Mech. Eng. Part D J. Automob. Eng.*, vol. 232, no. 3, pp. 367–383, 2018, doi: 10.1177/0954407017702986.

[17] M. Safari, S. J. Hosseinipour, and H. D. Azodi, "Experimental and Numerical Analysis of Forming Limit Diagram (FLD) and Forming Limit Stress Diagram (FLSD)," Mater. Sci. Appl., vol. 02, no. 05, pp. 496–502, 2011, doi: 10.4236/msa.2011.25067.

[18] M. R. Gheibi, M. H. Shojaeefard, and H. Saeidi Googarchin, "Experimental and numerical analysis on the cohesive behavior of an automotive adhesive improved by MWCNT subjected to mode I and II loadings," *Int. J. Mech. Sci.*, vol. 153–154, pp. 271–286, 2019, doi: 10.1016/j.ijmecsci.2019.02.009.

[19] B. Lu, J. Zhang, D. Zheng, T. Zhang, and J. Xie, "Energy absorption analysis on variable thickness CFRP/aluminum hybrid square tubes under oblique loading," *Int. J. Crashworthiness*, no. May, 2022, doi: 10.1080/13588265.2022.2074638.

[20] R. Kalhor, H. Akbarshahi, and S. W. Case, "Numerical modeling of the effects of FRP thickness and stacking sequence on energy absorption of metal-FRP square tubes," *Compos. Struct.*, vol. 147, pp. 231–246, 2016, doi: 10.1016/j.compstruct.2016.03.038.

[DOI: 10.22068/ase.2023.652]